IOP Publishing Semiconductor Science and Technology
Semicond. Sci. Technol. **30** (2015) 125004 (12pp) doi:10.1088/0268-1242/30/12/125004

Investigation of the possibilities of the 'saddle points' model for an explanation of anomalies in the characteristics of Schottky-barrier contacts

Anton V Shmargunov and Vladimir G Bozhkov

JSC 'Scientific Research Institute of Semiconductor Devices', 634034 Tomsk, Russia

E-mail: tohsh@list.ru

Received 11 June 2015, revised 15 September 2015
Accepted for publication 23 September 2015
Published 26 October 2015

Abstract

Numerical and experimental analyses of a model of a Schottky-barrier (SB) contact with barrier-height inhomogeneity in the form of 'saddle points' (the Tung model) [1] are carried out. On the basis of the known data for the contacts with Si, InP, and GaN and the experimental data obtained in this work for the Au–GaAs, Ni–GaAs, Ir–GaAs, and Pt–Rh–GaAs contacts, it is shown that the approximation widely used in the literature for the ideality factor of the *I*–*V* characteristics (IVCs) in the Tung model does not correspond to an exact solution, which, in turn, does not correspond to the real IVCs of contacts, at least at room temperature. The density of patches is demonstrated to have significant influence on the ideality factor under certain conditions, which is ignored by the Tung approximation. For the first time, on the basis of the known data on the distribution of the parameter γ (σ_γ), the spread of the barrier height (σ_φ) is simulated for a set of similar contacts. The results obtained indicate that the standard deviation σ_φ estimated on the basis of this model for the typical values of parameters significantly differs from the real values of σ_φ.

Keywords: Schottky barrier, inhomogeneity of the barrier height, dispersion of the barrier height, Tung model

(Some figures may appear in colour only in the online journal)

1. Introduction

In recent years, a model of inhomogeneity of the barrier height in the form of so-called 'saddle points' [1] is widely used to explain the IVC 'anomalies' of the metal–semiconductor contacts with the Schottky barrier. The popularity of this model, above all, is due its flexibility, that allows us, by selecting the model parameters, to explain the rather wide range of 'anomalies' of IVCs, including the well known 'low-temperature anomaly', first described in [2], as well as various kinds of IVC distortion at forward and reverse biases, the inverse relationship between the barrier height and ideality factor n of IVCs, and a few others.

According to [1, 3, 4], the 'saddle points' are formed as a result of a certain distribution of the barrier height over the contact area, where a region with relatively low barrier height and small area (the patch) is surrounded on all sides by a region with a barrier that is so high that a pinch-off of this first region occurs due to the lateral influence of the high-barrier region.

As a result, in this region, the potential barrier shape is significantly distorted: the maximum of the barrier height, exceeding that directly at the metal–semiconductor interface, is shifted deep into the semiconductor, and the top of the barrier acquires a rounded shape: that is, a 'saddle point' is formed.

The condition of formation of a 'saddle point' in the region (patch) with small barrier height and small (compared to the barrier width W) radius R_0 surrounded by a region with a relatively high barrier φ_b^0 can be represented in the form

[1, 4]

$$\frac{\Delta}{V_\varphi} > \frac{2R_0}{W}, \tag{1}$$

where $W \approx \left(2V_\varphi \eta\right)^{1/2}$ is the barrier width, $\eta \equiv \varepsilon_s/qN_D$, ε_s is the permittivity of the semiconductor, q is the electron charge, Δ is a decrease of the barrier height in the low-barrier region (at the metal–semiconductor interface), $V_\varphi = \varphi_b^0 - V - \varphi_s$ is the band bending in the high-barrier region, $q\varphi_s$ is the energy interval between the conduction band bottom and the Fermi level in the semiconductor, and V is the voltage (bias) on the barrier.

For the analysis of IVCs, an idea on the Gaussian distribution of these 'points' over the characteristic parameter γ is widely used [1]:

$$\begin{cases} N(\gamma) = \dfrac{2c}{\sqrt{2\pi}\,\sigma_\gamma} \exp\left(-\dfrac{\gamma^2}{2\sigma_\gamma^2}\right), \gamma \geqslant 0, \\ 0, \gamma < 0 \end{cases} \tag{2}$$

where

$$\gamma = 3\left(\frac{R_0^2\Delta}{4}\right)^{\frac{1}{3}}, \tag{3}$$

c is the patch density, and σ_γ is the standard deviation of the distribution of values of γ.

However, the wide spread of the Tung model, and even more its presentation as the only possible one, is not always justified. First of all, there is every good reason to believe that the probability of occurrence of regions with a 'normal' decrease of the barrier height (without the 'saddle point'), i.e. the probability of the condition reverse to equation (1), cannot be lower than the probability of the fulfillment of condition (1), since severe restrictions are imposed on this latter (see above). However, the regions that do not satisfy condition (1), and thus have lower barrier height than that in the 'saddle points' and larger areas, should determine the behavior of the IVC (especially the low-temperature behavior). Of course, this does not preclude situations where the effect of the regions with 'saddle points' can also be prominent due to the probabilistic nature of these effects.

An important argument of the authors of [1, 4] in favor of the determining role of 'saddle points' is the fact that these regions lead to the values of the IVC ideality factor greater than unity and to the well known 'low-temperature anomaly' of IVCs. However, the models of contacts with local thermionic-field emission [5, 6], with inhomogeneous energy distribution of the surface [7–10] and subsurface [10, 11] states in metal–semiconductor contacts, and with nonuniform distribution of the barrier height taking into account the effect of serial resistance [12, 13] also explain this and other 'anomalies' of IVCs. Moreover, in [8, 9, 14], these models and some others are combined on the basis of a more general model of the contact with nonlinear dependence of the barrier height on the bias voltage (this model is confirmed experimentally in a number of studies [10, 15–17]), as a universal cause of the low-temperature and other 'anomalies' of IVCs.

The purpose of this paper is the detailed numerical and experimental investigation of possibilities of the 'saddle point' model for an explanation of the various 'anomalies' in the SB-contact characteristics.

2. Analysis of the model

2.1. IVCs of an isolated patch

In accordance with the Tung model [1], the IVC of the contact is the sum of the currents through the individual patches with small barrier heights and the current through the homogeneous part of the contact with the barrier height φ_b^0. According to [1], the forward IVC of an individual patch can be represented as follows:

$$\begin{aligned} I_p &\approx R^*T^2\left(\frac{4\pi\gamma\eta^{2/3}}{9\beta V_\varphi^{2/3}}\right)\exp\left(-\beta\varphi_b^0 + \frac{\beta\gamma V_\varphi^{1/3}}{\eta^{1/3}}\right) \\ &\quad \times \exp(\beta V) \\ &= J_{idl}A_{pef}\exp\left(\beta\Delta\varphi_{bp}\right) \end{aligned} \tag{4}$$

where $J_{idl} = R^*T^2\exp\left(-\beta\varphi_b^0\right)\exp(\beta V)$ is the current density of a uniform (ideal) contact, R^* is the Richardson constant, T is the temperature, $\beta = q/kT$, A_{pef} is the effective patch area, $\varphi_{bp}(V) = \varphi_b^0 - \Delta\varphi_{bp}(V)$ is the patch barrier height, and $\Delta\varphi_{bp}$ is the decrease in the barrier height in the region of the patch:

$$A_{pef} = \frac{4\pi\gamma\eta^{2/3}}{9\beta V_\varphi^{2/3}}, \tag{5}$$

$$\Delta\varphi_{bp} = \frac{\gamma V_\varphi^{1/3}}{\eta^{1/3}}. \tag{6}$$

However, the barrier height $\varphi_{bp}(V)$ does not allow us to unambiguously describe the IVC of the patch, because of the strong dependence $A_{pef}(V)$. It is more convenient to introduce an effective barrier height φ_{pef} of the patch that takes into account the dependence $A_{pef}(V)$, as it is usually made for any real contacts with the characteristic, different from an ideal one [8, 12, 14]:

$$I_p = R^*T^2\left(\frac{4\pi\gamma\eta^{2/3}}{9\beta V_D^{2/3}}\right)\exp\left(-\beta\varphi_{pef}(V)\right)\exp(\beta V) \tag{7}$$

(here, the patch area at zero bias $V_D = \varphi_b^0 - \varphi_s = V_\varphi\big|_{V=0}$ is introduced). Then, for φ_{pef}, we obtain from the comparison of equations (7) and (4)

$$\varphi_{pef} = \varphi_b^0 - \Delta\varphi_{bp} - \frac{2}{3\beta}\ln\left(\frac{V_D}{V_\varphi}\right). \tag{8}$$

Further, based on the known expression for the IVC ideality factor [18], an individual patch can be characterized

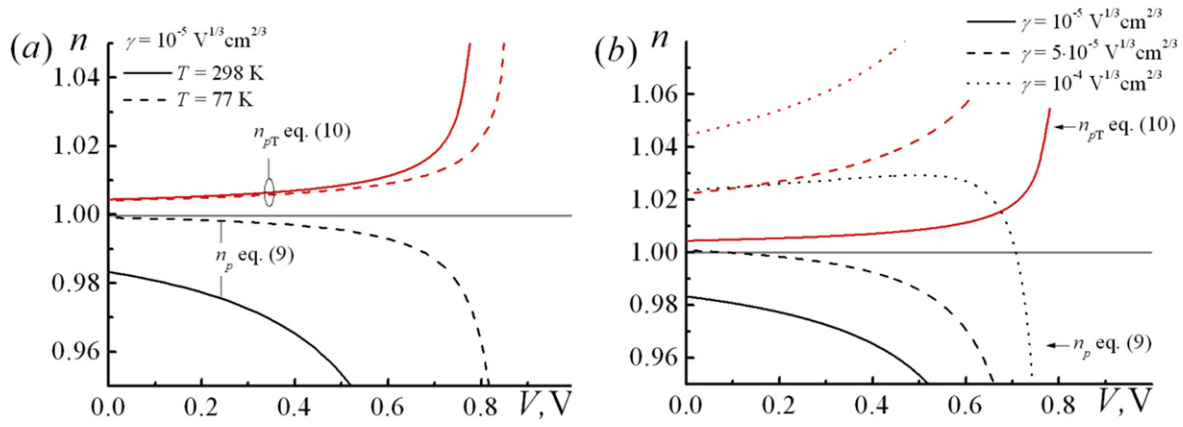

Figure 1. The dependences $n(V)$ for an isolated patch at different temperatures (*a*) and different values of γ at $T = 298$ K (*b*).

Table 1. Parameters of contacts and the calculated 'saddle point' model parameters.

Reference	Contact	N_D, cm^{-3}	A, cm^2	$n(T \approx 300$ K)	σ_γ,V$^{1/3}$ cm$^{2/3}$	c, cm^{-2}	φ_b^0, V
[1]	Si	10^{16}	—	1.06	6×10^{-5}	7×10^{10} ([a])	0.8
[20]	poly(pyrolle)–n-InP	5.2×10^{15}	0.13	1.02	5.8×10^{-5}	2.1×10^{10}	0.78
[21]	Sn–n-Si(111)-7 × 7	1.4×10^{15}	7.9×10^{-3}	1.41	2.18×10^{-4}	1.79×10^{7}	0.679
[22]	(1) Au–n-InP	7×10^{15}	—	1.04	4.9×10^{-5}	2×10^{10}	0.506
	(2) Cu–n-InP	10^{16}	—	1.06	4.85×10^{-5}	1.1×10^{10}	0.434
[25]	Au–Ni–GaN	10^{17}	10^{-3}	>1.4	10^{-4}	10^{7}	1.2

[a] Our estimate of the density of spots using the known ideality factor and other parameters of the model.

using the ideality factor in the following form:

$$n_p = \beta\frac{dV}{d\ln(I_p)} = \left(1 - \frac{d\varphi_{pef}}{dV}\right)^{-1} = \left(1 + \frac{2}{3\beta V_\varphi} - \frac{\gamma}{3\eta^{1/3}V_\varphi^{2/3}}\right)^{-1}. \quad (9)$$

Here, the second term in the brackets of the last expression is due to the bias dependence of the effective area of the patch and the third term is due to the bias dependence of the patch barrier height $\varphi_{bp}(V)$.

In the works of Tung and Sullivan [1, 4] and in subsequent papers by the majority of authors, for the IVC ideality factor of an individual patch, an approximation for small values of n is accepted, in which the contribution from the dependence $A_{pef}(V)$ is not taken into account.

$$n_{pT} \equiv \left(1 - \frac{\gamma}{3\eta^{1/3}V_\varphi^{2/3}}\right)^{-1} \approx 1 + \frac{\gamma}{3\eta^{1/3}V_\varphi^{2/3}}. \quad (10)$$

As it turns out, the use of this approximation gives an erroneous result. Figure 1(a) shows the dependences of the ideality factor on the bias voltage for different temperatures calculated according to the exact expression (9) and approximate expression (10) ($N_D = 10^{16}$ cm^{-3} and other parameters correspond to the GaAs contacts). The chosen value of the parameter $\gamma = 10^{-5}$ V$^{1/3}$ cm$^{2/3}$ is close to the maximum of the Gaussian distribution with $\sigma_\gamma \approx 5 \times 10^{-5}$ V$^{1/3}$ cm$^{2/3}$. This standard deviation lies in the range of values of the distribution dispersion most often observed in experiments (table 1).

A rather unexpected result is the appearance of the values $n < 1$ corresponding to the exact calculated value of the ideality factor according to equation (9). An increase in γ (figure 1(b)) promotes an increase in the values of n. At least two important conclusions follow from figure 1. First, the approximate and exact expressions for n give substantially different values. Second, the nature of the voltage dependence of the ideality factor of IVC of an individual patch equation (9) (an exact expression for the model of Tung) is not consistent with the known experimental results for IVCs of contacts with SBs [10, 15–17], where $n > 1$ and the ideality factor increases with the bias. Finally, the discrepancy between the exact equation (9) and approximate equation (10) is amplified by the fact that, at constant bias, the ideality factor increases according to the exact expression (9) with decreasing temperature. However, it decreases according to the approximate expression (10), figure 1(a). It is obvious that the difference between the dependences $n(V, T)$ for expressions (9) and (10) is due to the influence of the effective area of the patch, and this effect is surprisingly large. Moreover, this effect is opposite to the effect of the barrier height $\varphi_{bp}(V)$ of the patch and shows that the effective area of the patch increases with increasing bias and temperature, as shown in figure 2.

We note that, as mentioned above, the difference between the calculated (according to equation (9)) and experimental dependences $n(V)$ should be especially

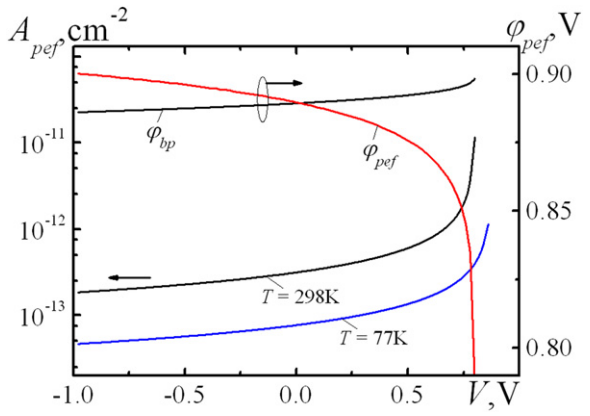

Figure 2. Voltage dependences of the effective area A_{pef} of an isolated patch at different temperatures and the effective barrier heights $\varphi_{\text{bp}} = \varphi_{\text{b}}^0 - \Delta\varphi_{\text{bp}}$ and φ_{pef} (8) at $T = 298$ K.

emphasized taking into account that in some papers (for example, in [1, 19, 20]), to describe the real IVC, a family of similar patches was used, which, as it turned out, is unacceptable.

As shown in figure 2, the barrier height of an individual patch $\varphi_{\text{bp}}(V) = \varphi_{\text{b}}^0 - \Delta\varphi_{\text{bp}}(V)$ increases nonlinearly with increasing bias, which is typical of real contacts with the SB [10, 15–17]. At the same time, the effective barrier height φ_{pef} of the patch determined according to equations (4), (7), and (8) decreases with increasing bias due to the contribution from the third term in equation (8) associated with the increase in the effective area of the patch $A_{\text{pef}}(V)$, which determines a negative slope of the dependence $n(V)$. The decrease in the effective area of the patch with decreasing temperature at given bias (in accordance with equation (5)) should result (in accordance with equation (9)) in an increase of the ideality factor, which is confirmed by figure 1(a).

2.2. IVC of a contact with the Gaussian distribution of the parameter γ

According to (2), for the Gaussian distribution of the characteristic parameter γ of patches, the current–voltage characteristic of the whole contact (the total IVC) can be represented in the following form [1]:

$$I_{\text{tot}} = I_{\text{idl}}\left\{1 + \frac{4}{9}\pi c\sigma_\gamma^2\left(\frac{\eta}{V_\varphi}\right)^{1/3}\exp\left(\frac{\beta^2\sigma_\gamma^2}{2}\left(\frac{V_\varphi}{\eta}\right)^{2/3}\right)\times\left[1 + \operatorname{erf}\left(\frac{\beta\sigma_\gamma}{\sqrt{2}}\left(\frac{V_\varphi}{\eta}\right)^{1/3}\right)\right]\right\}$$
$$= I_{\text{idl}}\left\{1 + f\exp\left(\frac{\beta^2\sigma_\gamma^2}{2}\left(\frac{V_\varphi}{\eta}\right)^{2/3}\right)\right\} = I_{\text{hom}} + I_{\text{inh}}. \quad (11)$$

Here, $I_{\text{idl}} = AJ_{\text{idl}}$—the ideal current, A is the total area of the contact, c is the patch density, and I_{hom} and I_{inh} are the currents of the homogeneous and inhomogeneous parts of the contact, respectively, that can be expressed in terms of the relative area of the inhomogeneous part of the contact A'_{inh} (see below).

$$I_{\text{hom}} = I_{\text{idl}}\left(1 - A'_{\text{inh}}\right), \quad I_{\text{inh}} = I_{\text{idl}}A'_{\text{inh}}\left(1 + Z_1\right). \quad (12)$$

Here,

$$\begin{cases} Z_1 = Z_2\sqrt{\pi}V_\varphi^{1/3}\exp\left(Z_2^2V_\varphi^{2/3}\right)\left[1 + \operatorname{erf}\left(Z_2V_\varphi^{1/3}\right)\right] \\ \approx 2Z_2\sqrt{\pi}V_\varphi^{1/3}\exp\left(Z_2^2V_\varphi^{2/3}\right), \\ Z_2 = \dfrac{\beta\sigma_\gamma}{\sqrt{2}\,\eta^{1/3}}. \end{cases} \quad (13)$$

The approximation in (13) corresponds to the condition $\operatorname{erf}\left(Z_2V_\varphi^{1/3}\right) = 1$ accepted in [1]. The value of f is represented as

$$f = \frac{4}{9}\pi c\sigma_\gamma^2\left(\frac{\eta}{V_\varphi}\right)^{1/3}\left[1 + \operatorname{erf}\left(\frac{\beta\sigma_\gamma}{\sqrt{2}}\left(\frac{V_\varphi}{\eta}\right)^{1/3}\right)\right] \approx \frac{8}{9}\pi c\sigma_\gamma^2\left(\frac{\eta}{V_\varphi}\right)^{1/3}. \quad (14)$$

In most cases, an approximation in equation (14) similar to that in equation (13) results in low error in the final result.

The second term in the curly brackets in equation (11) characterizes the excess current in an inhomogeneous contact (in comparison with I_{idl}) rather than the current of the inhomogeneous part of the contact I_{inh}. This means that the pre-exponential factor in the second term of the total IVC equation (11) (i.e. the value of f) does not correspond to the effective area of the inhomogeneous part A_{inh} of the contact, as is sometimes assumed [22], i.e. $f \neq A_{\text{inh}}$.

An exact expression for the effective area of the inhomogeneous part of the contact can be obtained by integration over the whole distribution of patches $N(\gamma)$ in the contact (2):

$$A_{\text{inh}} = AA'_{\text{inh}} = A\int_0^\infty N(\gamma)A_{\text{pef}}(\gamma)\,\mathrm{d}\gamma = \frac{4}{9}\frac{\sigma_\gamma c}{\beta}\sqrt{2\pi}\left(\frac{\eta}{V_\varphi}\right)^{2/3}. \quad (15)$$

Here, A_{inh} and A'_{inh} are the absolute and relative effective areas of the inhomogeneous part of the contact, respectively. This relation allows us to simultaneously obtain an effective area of the homogeneous part of the contact: $A_{\text{hom}} = A - A_{\text{inh}} = A(1 - A'_{\text{inh}})$.

As follows from (15) (see also figure 3), the total area of patches increases with their increasing density. Obviously, theoretically, a situation is not excluded where the relative effective area of patches is greater than unity, which is possible at $A_{\text{inh}} > A$. Physically, this means that the overlap of the effective areas of individual patches is possible, which is unacceptable according to the Tung model [1]. The model assumes that the individual patches are surrounded by areas with constant and relatively high barriers. Equation (15) allows us, using the condition $A'_{\text{inh}} < 1$, to introduce at least a

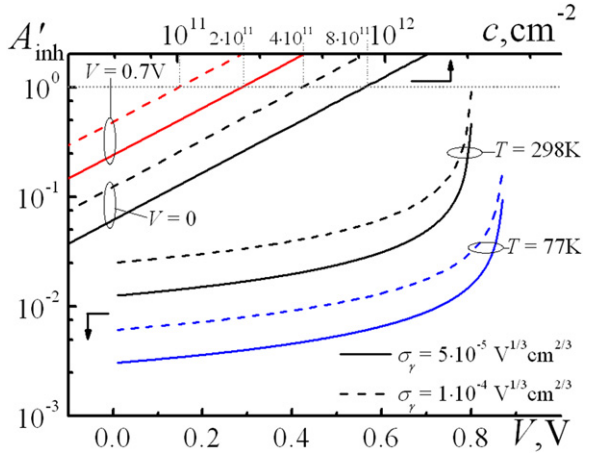

Figure 3. Bias and patch density (c) dependences of the relative effective total area of the inhomogeneous part of the contact A'_{inh} (15) (bias dependence at $c = 10^{10}\,cm^{-2}$); $N_D = 10^{16}\,cm^{-3}$.

rough criterion for the density of valid values of c absent from the model of Tung:

$$c < \frac{\pi}{4}\frac{9\beta}{4\sqrt{2\pi}\,\sigma_\gamma}\left(\frac{V_\varphi}{\eta}\right)^{2/3}. \tag{16}$$

Here, the factor $\pi/4$ corresponds to the uniform filling of the contact area by patches of a round shape. Clearly, this criterion depends on the applied bias, value of σ_γ, temperature, and concentration of doping impurity. According to equation (16), the maximum value of the density c is about $8 \times 10^{11}\,cm^{-2}$ at $\sigma_\gamma = 5 \times 10^{-5}\,V^{1/3}\,cm^{2/3}$ and $V = 0$ and about $2 \times 10^{11}\,cm^{-2}$ at $V = 0.7$ V (see figure 3). The value of the criterion is also affected by the uniformity of the patch distribution. In a real situation, due to the nonuniform distribution and arbitrary shape of patches, their overlap can occur at a much lower density than would be expected from equation (16). Like a patch (see (7)) or any other contact [8, 12, 14], the inhomogeneous contact can be characterized by an effective barrier height $\varphi_{bef}(V)$:

$$I_{tot} = AR^*T^2 \exp\left(-\beta\varphi_{bef}(V)\right)\exp(-\beta V). \tag{17}$$

It follows from the comparison of equations (11) and (17) that

$$\varphi_{bef}(V) = \varphi_b^0 - \beta^{-1}\ln\left(1 + f\exp\left(\frac{\beta^2\sigma_\gamma^2}{2}\left(\frac{V_\varphi}{\eta}\right)^{2/3}\right)\right). \tag{18}$$

According to the definition, the IVC ideality factor of an inhomogeneous contact is represented in a rather complicated form:

$$\begin{aligned} n_{tot} &= \beta\frac{dV}{d\ln(I_{tot})} = \left(1 - \frac{d\varphi_{bef}}{dV}\right)^{-1} \\ &= \left\{1 - \frac{A'_{inh}}{3\beta V_\varphi}\frac{\left[2Z_2^2V_\varphi^{2/3}(Z_1+1) - Z_1\right]}{1 + A'_{inh}Z_1}\right\}^{-1}. \end{aligned} \tag{19}$$

To understand what factors have the greatest effect on the value of n_{tot}, it is convenient to carry out a separate analysis of the effect of the inhomogeneous part of the contact. Taking into account the second expression in equation (12), the ideality factor of the inhomogeneous part of the contact with the area A_{inh} (total area of patches) takes the following form:

$$n_{inh} = \left(1 + \frac{2}{3\beta V_\varphi} - \frac{2}{3\beta V_\varphi}\left(\frac{Z_1}{2(1+Z_1)} + Z_2^2V_\varphi^{2/3}\right)\right)^{-1}, \tag{20}$$

where there is no dependence on the density of patches c.

Obviously, at $Z_1 \gg 1$ and Z_2 in accordance with equations (13), (20) can be transformed to the form

$$n_{inh} \approx \left(1 + \frac{1}{3\beta V_\varphi} - \frac{\beta\sigma_\gamma^2}{3\eta^{2/3}V_\varphi^{1/3}}\right)^{-1}, \tag{21}$$

that corresponds, as can be shown, to the ideality factor for an excess current of an inhomogeneous contact (see equation (11)). Finally, if in addition, a more stringent condition $A'_{inh}Z_1 \gg 1$ is fulfilled, an exact expression (19) for n_{tot} is transformed to the form (21) for n_{inh} of the inhomogeneous part of the contact.

In this case, as we can easily see, the influence of the area of the inhomogeneous part of the contact and density of patches on the value of n_{tot} is excluded (see equation(15)), and the role of the bias dependence of the effective barrier height of patches substantially increases. However, as for an individual patch (equation (9)), the bias dependence of the areas of patches still remains significant, judging by the presence of the second term in equation (21).

The Tung approximation, used by a number of researchers, follows from equation (21) by neglecting the second term, and we have

$$n_{totT} \approx 1 + \frac{\beta\sigma_\gamma^2}{3\eta^{2/3}V_\varphi^{1/3}}. \tag{22}$$

It should also be noted that, unlike the ideality factor for an inhomogeneous part of the contact (20), the ideality factor of the homogeneous part of the contact (not presented here) depends on the density of patches c, as can be shown using the first expression in equations (12) and (15).

2.3. Known experimental studies of the Tung model

To compare the calculation and experimental data, we use the known parameters of the 'saddle point' model taken from

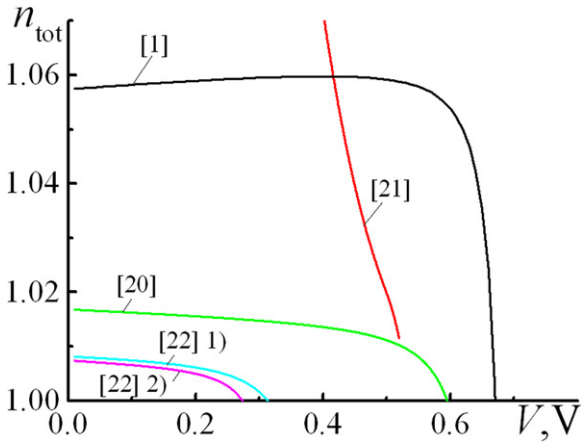

Figure 4. The dependence $n_{tot}(V)$ (19) for the model parameters from literature (table 1); $T = 298$ K.

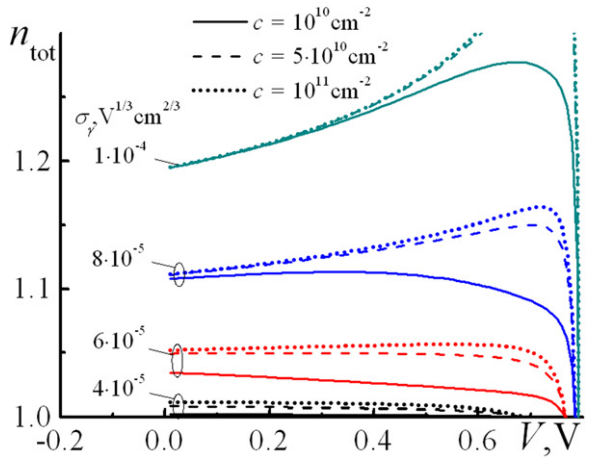

Figure 5. The dependences $n_{tot}(V)$ for $\sigma_\gamma = (4 \times 10^{-5}$–$10^{-4})$ V$^{1/3}$ cm$^{2/3}$ and $c = (10^{10}$—$10^{11})$ cm^{-2}; $T = 298$ K.

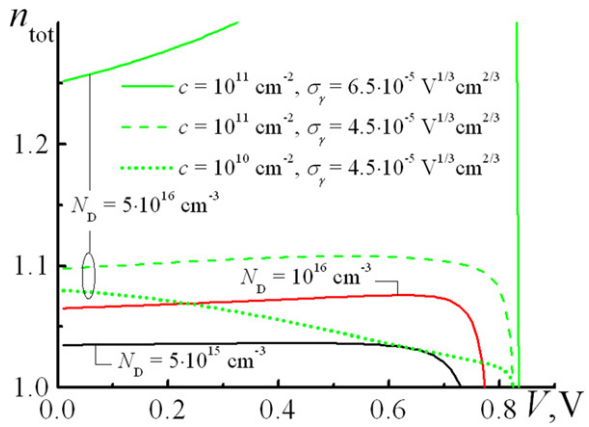

Figure 6. The dependences $n_{tot}(V)$ at different concentrations N_D; $T = 298$ K.

works presented in table 1. According to [1, 20–25], the standard deviation σ_γ is typically in the range of $(2 \times 10^{-5}$–$2 \times 10^{-4})$ V$^{1/3}$ cm$^{2/3}$. As can be seen, the lowest values of σ_γ correspond to the sufficiently perfect contacts (the IVC ideality factor $n < 1.1$), and the upper values correspond to the contacts with more substantial deviation of the ideality factor ($n > 1.2$).

For comparison, we selected the bias dependence of the ideality factor that, according to the experimental results [10, 15–17], is characterized by a positive slope, i.e. by an increase of the ideality factor with increasing bias.

Figure 4 shows the dependence $n_{tot}(V)$ calculated using equation (19) for the patch distribution parameters from table 1. The model parameters in table 1 were obtained as a result of fitting the exact IVC expression (11) to the experimental IVC. The used parameters of semiconductors (Richardson constant and permittivity) are shown in table 2. In the figure, there are no results of calculations made in accordance with the model parameters [25]. These results are characterized by very high values of n (>10) increasing with bias (at room temperature). As the figure shows, in general, the dependences $n_{tot}(V)$ are similar to those observed for the individual patches (figure 1): all of them are characterized by a decrease or by a weak increase of the values of n with increasing bias voltage followed by a drastic drop. All this means that the known results of calculations based on the model of 'saddle points' contradict the known experimental results. However, the absolute values of the ideality factor calculated according to equation (19) are, in general, close to the experimental values shown in table 1. The exceptions are the data of [25] characterized by higher values of the ideality factor.

Figures 5 and 6 give a better understanding of the influence of the parameters of the 'saddle point' model on the dependence $n_{tot}(V)$ (according to the above calculations using equation (19)). Figure 5 shows the bias dependence of the ideality factor for different values of σ_γ and c at $N_D = 10^{16}$ cm^{-3}. As can be seen, for small values of σ_γ (up to $\sigma_\gamma \sim 6 \times 10^{-5}$ cm^2), the ideality factors are small (less than

Table 2. Values of R^* and ε_s used in calculations.

Material	ε_s	R^*, A cm^{-2} K^{-2}
n-GaAs	13.1	8.156
n-Si	11.7	112
n-InP	12.5	9.4
n-GaN	8.9	26.9

1.05). The values of n decrease with increasing bias: more pronounced the smaller the density of patches. With increasing σ_γ, the values of n are substantially increased. Simultaneously, the slope of the dependence $n_{tot}(V)$ is changed from negative to positive (for a given value of c).

An increase in the density of patches c at a given σ_γ leads to a shift of the maximum of the dependence $n_{tot}(V)$ to higher positive values of bias (for small c, the maximum can be observed in the region $V < 0$). As a result, for high values of c, a positive slope is possible in this voltage range. In addition, the absolute value of the ideality factor is increased, although in this case an increase in n_{tot} is not as significant as that with increasing σ_γ.

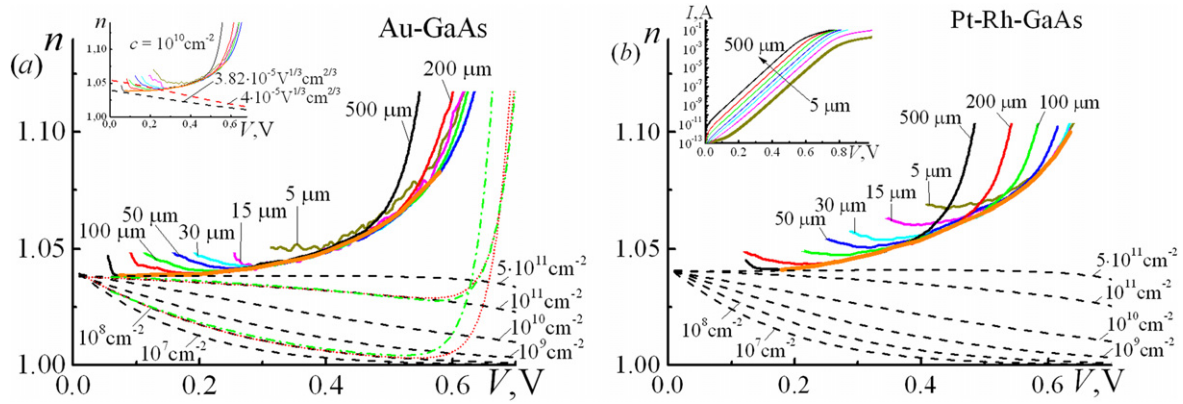

Figure 7. Experimental (solid lines) and calculated from (19) (dashed lines) dependences $n(V)$ for the contacts Au–GaAs (*a*) and Pt–Rh–GaAs (*b*) with the diameters of 500–5 μm. The calculation parameters are presented in table 4; dotted and dot–dashed lines correspond to calculations taking into account the series resistance in the integral current–voltage characteristic (11) and in the IVC of individual patches (4), respectively; $T = 298$ K.

The maximum of the dependence observed in figure 5 is, apparently, due to the imposition of the trend of growth of $n_{\rm tot}(V)$ typical of a certain combination of the model parameters, where the main role is played by the third term in equation (21), and the 'break' of the dependence $n_{\rm tot}(V)$ at high voltage is associated with the second term.

The impurity concentration in the semiconductor has a great influence on $n_{\rm tot}(V)$ (figure 6). An increase in the concentration (especially up to $N_{\rm D} = 5 \times 10^{16}$ cm^2) leads to a very sharp increase in the ideality factor. This effect is observed for various values of σ_γ and c.

In [1], it is also pointed out that the ideality factor increases with increasing concentration of doping impurity (with no allowance for tunneling). However, in this case, the calculated ideality factors are much higher than those observed experimentally. For example, according to the calculation (figure 6), at $N_{\rm D} = 5\times10^{16}$ cm$^{1/3}$ and $V = 0$ for σ_γ and c values in the range (4.5–4.6) $\times$ 10^{-5} V$^{1/3}$ cm$^{2/3}$ and (10^{10}–10^{11}) cm^{-2}, respectively, the value of n is in the range 1.08–1.25. These values are significantly higher than the experimental ones [26] and values calculated taking into account the tunneling current [14].

Theoretically, an increase in the concentration $N_{\rm D}$ can affect the distribution parameters of σ_γ and c. Thus, in accordance with criterion (1), an increase in the concentration of doping impurity may lead to the fact that some of the saddle points cannot be realized, causing a decrease in the values of c or σ_γ. However, it results in a negative slope of the voltage dependence of the ideality factor (figure 6).

2.4. Analysis of the experimental results obtained in the work

Although there are published data showing that the ideality factor of the contact IVC increases with the bias (see above), we conducted a special study of a number of contacts to obtain additional confirmation of this fact. Figures 7(a) and (b) show the experimental dependences of the ideality factor of the contacts Au–GaAs and Pt–Rh–GaAs, respectively, with the diameters of 500, 200, 100, 50, 30, 15, and 5 μm. The dependences $n(V)$ were calculated from the IVCs (see the inset in figure 7(b)). The dependences $n(V)$ for the GaAs contacts with Ni and Ir are similar [17]. Contacts were obtained by electrochemical deposition of metals on the epitaxial n-GaAs layers with the concentrations of 6×10^{16} cm^{-3} and 8×10^{16} cm^{-3}. Before the deposition of the metal, GaAs was etched in an NH_4OH:H_2O_2:H_2O = 10:3.5:500 solution for 15 s and dipped in NH_4OH:H_2O for 30 s. Solid lines are the averaged curves of the experimental data for a given diameter of the contact (for ten contacts with large diameters and up to 50 contacts with the diameters 5 μm); dotted lines are the data calculated in accordance with equation (19). Parameters of the experimental IVCs are given in table 3 ($\varphi_{\rm bm}$ is the barrier height measured using the saturation current (see equation (23)). Measurements of IVCs and processing of the results were performed with a probe station Cascade Microtech M150 using an Agilent B1500 semiconductor device analyzer.

Experimental dependences $n(V)$ of all the examined contacts show a definitely expressed positive slope (for example, in the Au–GaAs contacts, n increases from 1.038 at $V = 0.1$ V to 1.083 at $V = 0.6$ V). The plots for contacts with different diameters lie on a common curve, which, according to [10, 17], can be explained by the energy distribution of the density of interface states interacting with the semiconductor. This distribution is the same for each type of contact, regardless of its diameter. Deviations from this dependence at low bias voltages are caused by leaks affecting the ideality factor. Due to the fact that, for the contacts of different diameters, the leakages occur at different voltages, one can say that they are not related to the 'saddle points', since the dependence $n(V)$ in the Tung model is the same for all contact diameters. At large bias voltages, the influence of the series resistance is observed, also causing deviation from the general dependence. However, the character of the dependence $n(V)$ is undoubted.

Comparison between the experiment and calculation for the 'saddle point' model was performed as follows. At $V \to 0$, the ideality factor calculated according to equation (19) was fitted to the experimental values of n for

Table 3. Experimental values of the ideality factor and the measured barrier height at $I = 10^{-6}$ A.

Parameter of IVC at $I = 10^{-6}$ A	Au–GaAs	Ni–GaAs	Ir–GaAs	Pt–Rh–GaAs
n (500 μm)	1.045	1.051	1.067	1.049
n (5 μm)	1.084	1.101	1.12	1.083
φ_{bm}, V (500 μm)	0.834	0.785	0.889	0.838
φ_{bm}, V (5 μm)	0.809	0.761	0.867	0.829

fixed values of c: 5×10^{11}, 10^{11}, 10^{10}, 10^{9}, 10^{8}, and 10^{7} cm^{-2}. Fitting parameters are the values of σ_γ and φ_b^0. The results of fitting are shown in table 4. Further, the obtained fitting parameters were used to calculate the dependence $n_{tot}(V)$ over the entire range of bias voltages in accordance with equation (19).

The results presented in figure 7 demonstrate the fundamental difference between the experimental and calculated data. In contrast to the experimental dependences $n_{tot}(V)$, the calculated ones show a negative slope or a very weak positive dependence $n_{tot}(V)$. This result is quite expected, since it follows from the previous calculations presented in figures 4–6. The values of n are significantly different over the whole considered range of densities of patches. With increasing c, the calculated values of n approach the experimental ones, at least for small bias voltages. However, we cannot lose sight of the fact that, in this case, the values of c are beyond the reasonable values corresponding to condition (16), as shown in figure 3. As can be seen in the inset in figure 7(a), an increase in σ_γ at constant c results in an increase in the ideality factor. However, the negative slope of the dependence $n_{tot}(V)$ also increases.

A similar pattern is observed for the Pt–Rh–GaAs contacts (figure 7(b)) and contacts with Ni and Ir (not shown here). Thus, for all the contacts considered, the 'saddle point' model gives results that do not match the real dependence $n(V)$.

One of the formal factors that can lead to an increase in the ideality factor with increasing bias is the effect of the series resistance of the contact. In [21], the resistance in the Tung model was taken into account by replacing the term $V_\varphi = \varphi_b^0 - \varphi_s - V$ in the expression for the total current equation (11) by the term $V'_\varphi = \varphi_b^0 - \varphi_s - V + IR_s$. The permissibility of such a replacement is not obvious, since strictly speaking such an inclusion of the resistance should be done for the IVC of each of the patches of the contact, and then these characteristics should be summed. This calculation was performed. The calculation technique is similar to that used in section 2.5 of this paper.

The area of the patch was calculated in accordance with equation (5). It should be noted that A_{pef} is also a function of bias, and to simplify the calculation the influence of R_s was not considered in this case. In our opinion, this should not lead to a large error.

Calculations made for two values of the density of patches, $c = 10^{11}$ cm^{-2} and $c = 10^{8}$ cm^{-2}, for Au–GaAs contacts (figure 7(a)) allow to draw the following conclusions. First, the account of the dependence of the total current on the value of R_s according to [21] provides a result close to that obtained by considering the effect of the spreading series resistance on the IVC of each of the patches, especially at high densities c. Second, the Tung model, taking into account the series contact resistance according to [21] and the spreading resistance of patches (and without taking them into account), fails to adequately describe the experimental characteristics. The effect of the resistance is pronounced at sufficiently high voltages (~0.6 V). At lower bias voltages, the calculated dependence $n(V)$ has a negative slope.

Besides the barrier-height inhomogeneity and existence of interface states, the dipole interfacial layer can influence electrical characteristics of the SB contact, which was observed in [27] for an electrochemically deposited contact. This can lead to a remarkable increase of the barrier height in Au–GaAs contacts (up to ~1 V). However, it should be kept in mind that in [27] the finishing treatment included etching in a solution of H_2SO_4 followed by etching in a solution of HCl. According to [28], the H_2SO_4 and HCl treatments leave a great many oxide complexes on the GaAs surface (such as Ga_2O_3, As_2O_3). The ammonia treatment leaves a smaller number of such complexes on the surface. This may be the reason for the smaller barrier height—0.834 V in our case (see table 1). Thus, we can conclude that the effect of the dipole layer on the barrier height in this work is not so high. As for the influence of the dipole layer on the $n(V)$ behavior, we have no results that confirm such a possibility.

It seems amazing that with such a significant difference between the exact calculated and experimental dependences of the ideality factor $n(V)$ (figures 7(a) and (b)), the Tung approximation in the form (22) has found rather wide use in practical analysis [1, 22, 29] of IVCs of contacts. Figures 8(a)–(c) partly help to explain this fact. In these figures, a comparison is made of the exact (equation (19)) and approximate (equation (22)) values of the ideality factor for the contact with Si [1] (table 1, figure 4) and the Au–GaAs contact (figure 7(a)). The parameters of the contacts (σ_γ and c) are shown in the figures. Figures 8(a) and (b) correspond to high values of the parameter c and figures 8(c) and (d) correspond to relatively low values of c. The values of σ_γ (see table 1) correspond to the relatively low values, which are usually implemented for sufficiently perfect contacts. In figure 8, an assessment of the influence of the approximation erf = 1 on the ideality factor is also given for the conditions used. This assessment also confirms the acceptability of this approximation.

Figure 8(a) shows that, at room temperature, there is neither qualitative nor quantitative agreement between the exact and approximate values of n. The difference between these values is similar to the difference between them for a single patch (figure 1). However, at low temperature (figure 8(b)), the qualitative difference disappears, there is only a quantitative one. It depends on the parameters of the model, but nevertheless it is observed over a broad range of values of the parameters σ_γ and c and for various barrier heights.

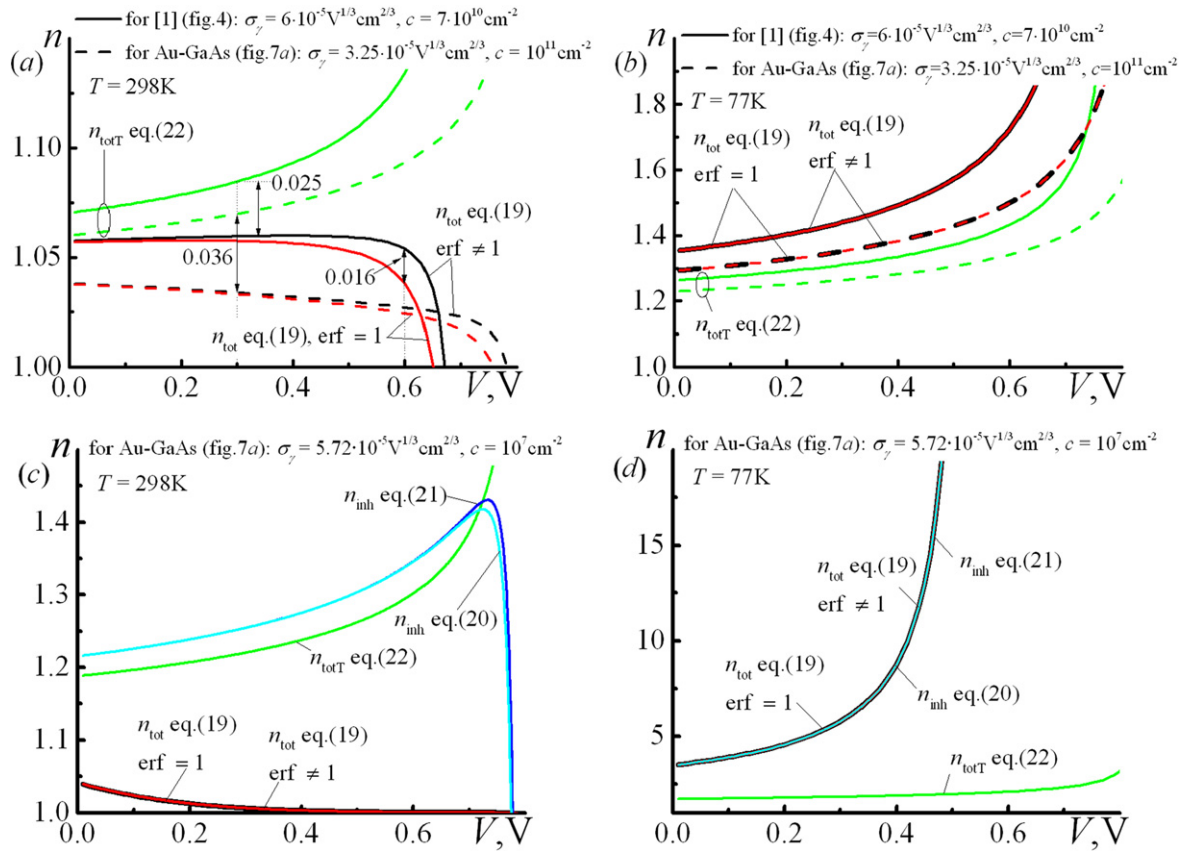

Figure 8. The dependences $n_{tot}(V)$ (19), n_{inh} (20), n_{inh} (21), and n_{totT} (22) at $T = 298$ K (a, c) and $T = 77$ K (d, e) for the model parameters from [1] (table 1) and for Au–GaAs at $c = 10^{11}$ cm^{-2} (table 4) (a, b) and model parameters for Au–GaAs at $c = 10^{7}$ cm^{-2} (table 4) (c, d).

Table 4. Values of parameters of the Tung model used in the calculation of fitting dependences.

	Au–GaAs		Ni–GaAs		Ir–GaAs		Pt–Rh–GaAs	
c, cm^{-2}	σ_γ, V$^{1/3}$ cm$^{2/3}$	φ_b^0, V	σ_γ, V$^{1/3}$ cm$^{2/3}$	φ_b^0, V	σ_γ, V$^{1/3}$ cm$^{2/3}$	φ_b^0, V	σ_γ, V$^{1/3}$ cm$^{2/3}$	φ_b^0, V
5×10^{11}	3×10^{-5}	0.893	2.9×10^{-5}	0.845	2.9×10^{-5}	0.958	3.05×10^{-5}	0.898
10^{11}	3.25×10^{-5}	0.871	3.05×10^{-5}	0.817	3.1×10^{-5}	0.935	3.3×10^{-5}	0.876
10^{10}	3.85×10^{-5}	0.857	3.58×10^{-5}	0.803	3.6×10^{-5}	0.916	3.83×10^{-5}	0.859
10^{9}	4.45×10^{-5}	0.851	4.18×10^{-5}	0.797	4.15×10^{-5}	0.91	4.47×10^{-5}	0.852
10^{8}	5.1×10^{-5}	0.847	4.77×10^{-5}	0.794	4.68×10^{-5}	0.906	5.11×10^{-5}	0.848
10^{7}	5.72×10^{-5}	0.844	5.345×10^{-5}	0.792	5.22×10^{-5}	0.903	5.72×10^{-5}	0.847

The difference between the approximate and exact values of the ideality factor is especially great at relatively low densities of patches (figures 8(c) and (d)). An unconditional contribution to this effect is made by the fact that an approximate equation (22) does not take into account the dependence on c. Therefore, the ideality factor of the inhomogeneous part of the contact n_{inh} (equation (20)), also independent of the density of spots at room temperature (figure 8(c)), is much closer to the approximate expressions (21) and (22) than to the exact expression for n_{tot} (19) depending on c. We also note that, as shown in figure 8(c), equation (20) is almost equal to its simplified approximation of equation (21). Finally, we can add to the above that the 'saddle point' model in the approximation of Tung at relatively small values of c (10^{7}–10^{8} cm^{-2}) used in [21, 25] for the analysis of current–voltage characteristics of real SB contacts seems to be not justified.

A characteristic pattern is observed at low (77 K) temperature (figure 8(d)). Coincidence of the results for n obtained using equations (19)–(21) means that, in this case, the main role is played by the second term in equation (21) caused by the dependence of the effective area of patches on the bias (equation (15)). This term is absent from the Tung approximation (22), which determines its significant difference from the approximations (20) and (21) and the exact solution (19).

Considering the temperature dependence of the IVC parameters as a whole (in the model of Tung), at least for

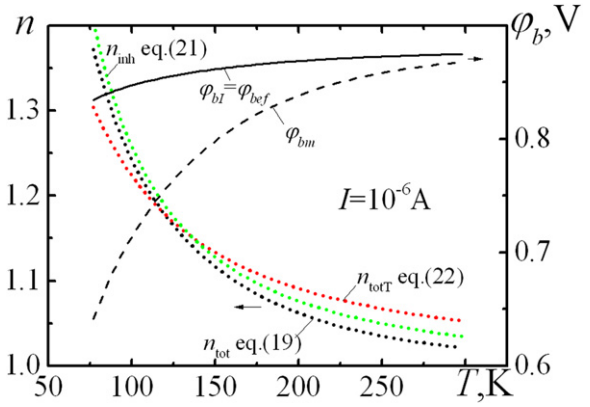

Figure 9. Temperature dependences of n_{tot} (19), n_{inh} (21), n_{totT} (22), φ_{bm}, and$\varphi_{bI} = \varphi_{bef}|_{I=const}$.

sufficiently perfect contacts (relatively low values of dispersion $\sigma_\gamma = 5 \times 10^{-5}\,V^{1/3}\,cm^{2/3}$) and, in contrast, for sufficiently high values of patch density ($c = 5 \times 10^{10}\,cm^{-2}$), this dependence may correspond to a low-temperature anomaly, as shown in figure 9. With decreasing temperature, the values of n are increased and the barrier height φ_{bm} measured at a current of $I = 10^{-6}$ A and calculated directly from the IVC (11) is decreased:

$$\varphi_{bm}(V) = \beta^{-1}\ln\left(\frac{AR^*T^2}{I_{Sn}}\right) = \beta^{-1}\ln\left(\frac{AR^*T^2}{I}\right) + \frac{V}{n}. \tag{23}$$

The effective barrier height (equation (18)) introduced when comparing equations (11) and (17), which also may be determined directly from the IVC according to the expression

$$\varphi_{bef}(V) = \beta^{-1}\ln\left(\frac{AR^*T^2}{I}\right) + V, \tag{24}$$

at constant current ($I = 10^{-6}$ A, $\varphi_{bef}|_{I=const} \equiv \varphi_{bI}$), also decreases with increasing temperature. This distinguishes the 'saddle point'model from the model of an ideal contact taking into account the tunneling and image force effects [14].

Figure 9 shows the comparison of the dependences $n_{tot}(T)$ for the exact solution (19), the approximation of Tung (22), and the approximation proposed in this paper for the inhomogeneous part of the contact (21). The latter is much closer to the exact value than the approximation of Tung, because it takes into account the two factors affecting the ideality factor, the changes in area of the patches and the effective barrier height, while in the approximation of Tung only the second factor is considered. Another interesting fact is that the sign of the relationship between the exact value of n and the approximation of Tung is changed, which indicates the change in the role of the effective contact area and the effective barrier height in the change of n with decreasing temperature.

2.5. Modeling the barrier-height dispersion on the basis of the data for σ_γ

The dispersion of the barrier height is one of the most important parameters of real contacts indicating the contact perfection. However, in the 'saddle point' model, it remains in the 'shadow' of the dispersion of the characteristic parameter of 'saddle points' γ, and it is difficult to tell anything definite about it. In this paper, the first attempt is made to evaluate the dispersion of the barrier height using the known parameters of the Gaussian distribution of γ (σ_γ and c) and thus to compare it with the experimental data. Such a comparison may be an additional argument in favor of the 'saddle point' model, or against it. Concretely speaking, we are talking about assessing the effect of the standard deviation σ_γ, density of patches c, and concentration of doping impurity on the standard deviation of the barrier height σ_φ.

Initial parameters of the Gaussian distribution of the parameter γ (σ_γ and c) were selected from the data given in table 1. Parameters of the materials were chosen from table 2. The problem was reduced to the simulation of a random parameter γ in the range from 0 to $5\sigma_\gamma$ using a pseudo-random number generator (PRNG) modified to obtain the Gaussian distribution. To determine the dispersion σ_φ, at least 50 such arrays should be ontained for each of the contacts. The procedure for formation of the IVC of the contact included the construction of an IVC corresponding to each patch of the array, i.e. to each value of γaccording to equations (4) and (5), followed by their summation and taking into account the IVC of the homogeneous part of the contact. The area of this part was determined as the difference between the total area of contact and the effective area of the patches. For each of the 50 IVCs of the contacts, the barrier height measured at a current of 10^{-6} A was determined. Then, the standard deviation of the barrier height σ_φ was determined. Further, these values obtained on the basis of the model of Tung were compared with the known experimental data. In our experiments, the standard deviations of φ_{bm} were determined for IVCs of the Au–GaAs, Ni–GaAs, Ir–GaAs, and Pt–Rh–GaAs contacts (30 contacts of each diameter).

The results of the simulation are shown in figure 10. The figure also shows the experimental value of the standard deviation of the barrier height taken from a number of works, including those obtained in the present study. We note that the comparison was made for contacts which have almost the same perfection: the experimental ideality factors of contacts with Ir, Au, Ni, and Pt–Rh obtained in this study (table 3, figure 7), the known experimental data [24, 30–32], and the results of studies used for the calculations ([1, 20, 22], table 1) are practically identical. Only the data from [21, 25], where the ideality factor is greater than 1.2, should be allocated.

Attention should be paid to the weak dependences of the dispersion on the diameter of the contact and even its slight decrease for small contact diameters according to [21] and [25]. In this case, the special features and 'fluctuations' of the dependence $\sigma_\varphi(d)$ may be associated with the low density of patches ($c \sim 10^7\,cm^{-2}$), which leads to the fact that the contacts of small diameters (<30 μm) contain only a few

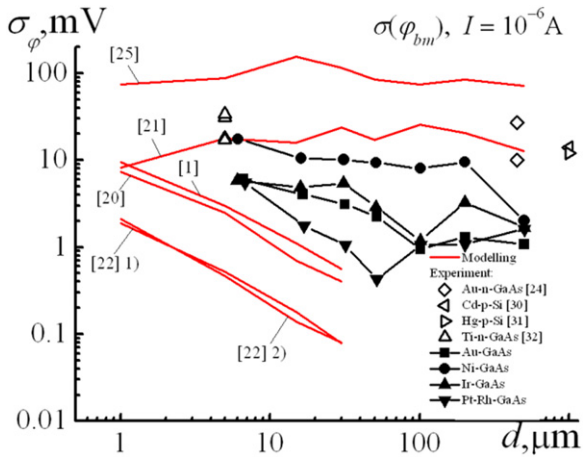

Figure 10. Dependences of the standard deviation of the barrier height σ_φ, measured using the saturation current, on the diameter of the contact (at $I = 10^{-6}$ A): solid lines, calculation; symbols, known experimental data; lines with symbols, experimental results obtained in this work. Model parameters for the calculation are taken from table 1; $T = 298$ K.

patches. For example, for the model parameters from [21], an average number of patches in the contact with the diameter of 5 μm is about 3.5. Therefore, in this case, it is difficult to assess Gaussian distribution. The values of the standard deviation for these model parameters are quite high (10–100 mV). This is due to the high value of $\sigma_\gamma \sim 10^{-4}\,\mathrm{V}^{1/3}\,\mathrm{cm}^{2/3}$. Once again, we note that for such values of σ_γ the ideality factor is greater than 1.2.

The remaining calculated dependences $\sigma_\varphi(d)$ corresponding to [1, 20, 22] have expected slopes; i.e., the dispersion increases with decreasing diameter of the contact. However, the values of the dispersion are, in general, very small. The calculated results approach the experimental ones only for the contacts with diameters of 5 μm ($\sigma_\varphi = 3$mV) [1]. For the contacts with large diameters, the difference is significant and can reach two orders of magnitude. This difference increases with increasing diameter. Obviously, the results of the comparison do not testify in favor of the 'saddle point' model.

3. Conclusions

A calculation analysis of the 'saddle point' model has been carried out. This model is widely used to explain the 'anomalies' of characteristics of the SB contacts with the SB. The main objects of the research were the ideality factor, the effective and measured barrier height, and their dependences on the bias and temperature. An exact expression for the ideality factor of the contact with the Gaussian distribution of patches and a number of approximations are obtained.

The features of the contributions from the homogeneous and inhomogeneous parts of the contacts to the IVC ideality factor are analyzed and the limit density of patches, at which they completely fill the contact area, is evaluated. The influence of the standard deviation σ_γ of the patch distribution, density of patches c, and doping level on the behavior of ideality factor is investigated.

It is shown that, depending on the values of σ_γ, c and N_D and their combinations, the values of n and the slopes of the dependences $n_\mathrm{tot}(V)$ may vary considerably. The character of the bias dependences of these quantities is usually not consistent with that observed experimentally.

The most significant result of the analysis is that the used approximations of the Tung model [1] for the values of the ideality factor of an individual patch and the ideality factor of the contact with the Gaussian distribution over γ are not consistent, and often contradict the exact calculated expressions for the ideality factor. The exact values of n also significantly (fundamentally) differ from the experimental values for the contacts with Au, Ni, Ir, and Pt–Rh with GaAs at high (room) temperature.

However, at low temperature, a sufficient consistence of the exact and approximate values of n increasing with decreasing temperature is observed, and the measured barrier height is decreased therewith, as expected from the experiment. This correspondence is observed at sufficiently large ($>10^{10}\,\mathrm{cm}^{-2}$) densities of patches, but at low densities of patches ($\sim 10^{7}\,\mathrm{cm}^{-2}$) it is absent. There is a significant difference between the exact and approximate (Tung's) expressions for the ideality factor at low and room temperatures in this case.

On the basis of the known experimental parameters of the 'saddle point' model (standard deviation σ_γ, density of patches c, barrier height, and concentration of doping impurity), the standard deviation σ_φ of the barrier height was simulated for various diameters of contacts. A comparison of these values with the experimental values is performed. It is shown that the absolute values of the simulated standard deviation (for the characteristics with $n < 1.1$) and the character of the dependences $\sigma_\varphi(d)$ (for $n > 1.2$, $\sigma_\gamma \sim 10^{-4}\,\mathrm{V}^{1/3}\,\mathrm{cm}^{2/3}$, $c \sim 10^{7}\,\mathrm{cm}^{-2}$) significantly differ from the experimental data. The values of σ_φ calculated in this way represent an additional parameter of IVCs that can be used (along with the ideality factor and barrier height) to test the 'saddle point' model for compliance with the experiment.

The Tung model explains some features of IVCs of real SB contacts. However, it should be applied with caution, especially to the experimental results obtained at room temperature. And, of course, it cannot be used for comprehensive explanation of all the anomalies of the IVCs. In our opinion, a model of the contact with the nonuniform energy distribution of the surface and subsurface states may be supposed, as an alternative. This model is detailed in [10, 17] and experimentally confirmed by atomic force microscopy data [33]. However, the effect of the barrier-height inhomogeneity, in one form or another, cannot be excluded, especially at low temperatures.

Acknowledgments

The authors would like to express their thanks to the technological department of JSC 'Scientific Research Institute of

Semiconductor Devices' and especially to A I Orekhova for preparation of samples and T P Bekezina for electrochemical deposition of Ir.

References

[1] Tung R T 1992 Electron transport at metal–semiconductor interfaces: general theory *Phys. Rev.* B **45** 13509

[2] Padovani F A and Sumner G G 1965 Experimental study of gold–gallium arsenide Schottky barriers *J. Appl. Phys.* **38** 3744

[3] Bastis A Y, Bikbaev V B, Vaytkus Y Y and Karpinskas S C 1988 *Lithuanian Phys. Collection* **28** 191

[4] Sullivan J P, Tung R T, Pinto M R and Graham W R 1991 Electron transport of inhomogeneous Schottky barriers: a numerical study *J. Appl. Phys.* **70** 7403

[5] Bozhkov V G and Kurkan K I 1979 *Sbornik nauchnykh trudov: Poluprovodnikovye pripory s baryerom Shottki* (Kiev: Naukova dumka) p43

[6] Bozhkov V G and Kashkan A A 1981 *Elektron. Tekhn., Ser. 2, Poluprovodn. Prib.* No.7(150) 12

[7] Bozhkov V G 1987 *Izv. Vuzov. Fiz.* **2** 29

[8] Bozhkov V G 2002 On the nature of the 'Low-Temperature Anomaly' in metal–semiconductor Schottky-Barrier contacts *Radiophys. Quantum Electron.* **45** 381

[9] Bozhkov V G and Kuzyakov D J 2002 Low-frequency noise and current–voltage characteristics of Schottky barrier contacts in a wide temperature range *J. Appl. Phys.* **92** 4502

[10] Bozhkov V G and Shmargunov A V 2012 Investigation of special features of parameters of Schottky barrier contacts caused by a nonlinear bias dependence of the barrier height *J. Appl. Phys.* **111** 053707

[11] Bozhkov V G and Zaitzev S E 2005 *Russ. Phys. J.* **48** 1085

[12] Bozhkov V G and Zaitzev S E 2007 *J. Commun. Technol. Electron.* **52** 87

[13] Chand S and Kumar J 1996 On the existence of a distribution of barrier heights in Pd_2Si/Si Schottky diodes *J. Appl. Phys.* **80** 288

[14] Bozhkov V G and Shmargunov A V 2011 Influence of nonlinear bias dependence of the barrier height on measured Schottky barrier contact parameters *J. Appl. Phys.* **109** 113718

[15] Newman N, Van Schilfgaarde M, Kendelewicz T, Williams M D and Spicer W R 1986 Electrical study of Schottky barriers on atomically clean GaAs(110) surfaces *Phys. Rev.* B **33** 1146

[16] Sehgal B K, Balakrishnan V R, Gulati R and Tewari S P 2003 *J. Semicond. Technol. Sci.* **3** 1

[17] Bozhkov V G, Shmargunov A V, Bekezina T P, Torkhov N A and Novikov V A 2014 The Ir–n-GaAs Schottky barrier contacts made by electrochemical deposition *J. Appl. Phys.* **115** 224505

[18] Rhoderick E H and Williams R H 1988 *Metal–Semiconductor Contacts* 2nd edn (Oxford: Clarendon)

[19] Roccaforte F, La Via F, Raineri V, Pierobon R and Zanoni E 2003 Richardson's constant in inhomogeneous silicon carbide Schottky contacts *J. Appl. Phys.* **93** 9137

[20] Jones F E, Wood B P, Myers J A, Daniels-Hafer C and Lonergan M C 1999 Current transport and the role of barrier inhomogeneities at the high barrier n-InP/poly(pyrrole) interface *J. Appl. Phys.* **86** 6431

[21] Schmitsdorf R F, Kampen T U and Monch W 1997 Explanation of the linear correlation between barrier heights and ideality factors of real metal–semiconductor contacts by laterally nonuniform Schottky barriers *J. Vac. Sci. Technol.* B **15** 1221

[22] Çetin H, Sahin B, Ayyldiz E and Türüt A 2004 The barrier-height inhomogeneity in identically prepared H-terminated T/p-Si Schottky barrier diodes *Semicond. Sci. Technol.* **19** 1113

[23] Leroy W P, Opsomer K, Forment S and Van Meirhaeghe R L 2005 The barrier height inhomogeneity in identically prepared Au/n-GaAs Schottky barrier diodes *Solid-State Electron.* **49** 878

[24] Biber M, Güllü Ö, Forment S, Van Meirhaeghe R L and Türüt A 2006 The effect of Schottky metal thickness on barrier height inhomogeneity in identically prepared Au/n-GaAs Schottky diodes *Semicond. Sci. Technol.* **21** 1

[25] Sarpatwari K, Mohney S E and Awadelkarim O O 2011 Effects of barrier height inhomogeneities on determination of the Richardson constant *J. Appl. Phys.* **109** 014510

[26] Broom R F, Meier H P and Walter W 1986 Doping dependence of the Schottky-barrier height of Ti–Pt contacts to n-gallium arsenide *J. Appl. Phys.* **60** 1832

[27] Forment S, Van Meirhaeghe R L, De Vrieze A, Strubbe K and Gomes W P 2001 *Semicond. Sci. Technol.* **16** 975–81

[28] Bekezina T P and Mokrousov G M 2000 *Inorg. Mater.* **36** 857

[29] Lucolano F, Roccaforte F, Giannazzo F and Raineri V 2007 *Appl. Phys. Lett.* **90** 092119

[30] Akkiliç K, Türüt A, Çankaya G and Kiliçoğlu T 2003 *Solid State Commun.* **125** 551

[31] Wittmer M and Freeouf J L 1992 *Phys. Rev. Lett.* **69** 2701

[32] Forment S, Biber M, Van Meirhaeghe R L, Leroy W P and Türüt A 2004 *Semicond. Sci. Technol.* **19** 1391

[33] Shmargunov A V, Bozhkov V G and Novikov V A 2015 *Microelectron. Eng.* **133** 73